Int. J. Multiphase Flow Vol. 17, No. 1, pp. 77–94, 1991
Printed in Great Britain.

0301-9322/91 $3.00 + 0.00

A PHENOMENOLOGICAL MODEL OF SUBCOOLED FLOW BOILING IN THE DETACHED BUBBLE REGION

J. Y. YANG† and J. WEISMAN
University of Cincinnati, Cincinnati, OH 45211, U.S.A.

(Received 29 May 1990; in revised form 20 September 1990)

Abstract—The Weisman–Illeslamlou model for the critical heat flux in subcooled boiling has been extended to the determination of boiling heat fluxes throughout the detached bubble region. Both the original model and its extension are based on the assumption that turbulent interchange at the edge of the bubbly layer on the heated wall is the limiting process. By recognizing that the turbulent intensity at the bubbly layer edge is a function of the bubbly layer void fraction, the relationship between heat flux and bubbly layer quality can be established. The bubbly layer quality so obtained allows the computation of the fraction of heat transferred by boiling. With the additional assumption that the wall temperature and boiling heat flux are uniquely related, the wall temperature may be calculated. The boiling curves obtained are shown to be in reasonable agreement with data for subcooled boiling of refrigerant 113 in round tubes. The extended theory is also shown to provide predictions of the onset of the detached bubble region.

Key Words: heat transfer, subcooled boiling, nucleate boiling, critical heat flux, bubble detachment.

1. INTRODUCTION

In a heated tube in which there is subcooled boiling of an internal liquid coolant, a forced convection region is typically found near the tube inlet. This is followed by a boiling region in which nearly all bubbles are attached to the heated surface while they grow and collapse. The "attached bubble" region is succeeded by a region in which vapor bubbles are released from the wall although the bulk liquid temperature is still below saturation. While some of the released bubbles are condensed, some remain and there is net vapor generation. This "detached bubble" region is the subject of the present paper.

Weisman & Pei (1983) previously developed a phenomenologically based model for the critical heat flux at (CHF) at low qualities and moderate subcooling. Weisman & Ying (1985) extended the model to higher qualities and lower flow rates. Subsequently, Ying & Weisman (1986) applied the model to rod bundles. Most recently, Weisman & Illeslamlou (1988) modified the CHF model so that it could be applied to high subcoolings and thus cover the entire detached bubble region. In this work, we consider how this theory may be extended to heat fluxes below the CHF. Some new data, which can be compared to the proposed approach, are also presented.

2. ORIGINAL CHF MODEL

Based on the photographic observations of Jiji & Clark (1964) and Tong *et al.* (1965), the previously developed CHF model (Weisman & Pei 1983) assumes the existence of a bubbly layer adjacent to the heated surface. Within the bubbly layer, the scale of turbulence is too small for the turbulent eddies to affect the vapor bubbles. The outer edge of the bubbly layer occurs when the eddy size is sufficiently large to influence the bubbles. It is assumed that the turbulent interchange at the edge of the bubbly layer limits the total rate of heat transfer. Weisman & Illeslamlou (1988) therefore wrote an energy balance at the bubbly layer edge and obtained

$$q'' = G'(h_2 - h_1) = G\psi i_b(h_2 - h_1), \qquad [1]$$

†Current address: Department of Chemical and Nuclear Engineering, University of New Mexico, Albuquerque, NM 87131, U.S.A.

where

G' = lateral mass velocity from the core to the bubbly layer due to turbulence (mass/area time),
h_2, h_1 = bubbly layer and core fluid enthalpies, respectively (energy/mass),
q'' = total heat flux (energy/area time)

and

ψ = parameter defined by [4].

The turbulent intensity, i_b, is evaluated at the bubbly layer edge which is taken as the location where the Prandtl mixing length (an index of the scale of turbulence) is K times the bubble diameter. After fitting the single-phase turbulent intensity curve of Lee & Durst (1980) with a simple curve, the turbulent intensity was found to be given by

$$i_b = 0.462(K)^{0.6}(\mathrm{Re})^{-0.1}\left(\frac{D_b}{D}\right)^{0.6}\left[1 + \frac{a(\rho_L - \rho_G)}{\rho_G}\right], \quad [2]$$

where

D = tube diameter (length),
D_b = bubble diameter (length),
Re = Reynolds number based on total mass flow and liquid properties

and

ρ_G, ρ_L = gas and liquid phase densities, respectively (mass/volume).

The parameter "K" was empirically determined to be 2.5. The term $[1 + a(\rho_L - \rho_G)/\rho_G]$ represents an empirical correction to the single-phase turbulent intensity to allow for the presence of vapor bubbles. The parameter "a" is an empirical constant fixed at 0.135 for any mass fluxes $\leqslant 9.7 \times 10^6\ \mathrm{kg/m^2\,h}$ and a superficial liquid velocity > 1.36 m/s. The bubble diameter, D_b, was based on a slight modification of Levy's (1967) approach and is given by

$$D_b = \left[0.015\left(\frac{\sigma D_h}{\tau_w}\right)^{1/2}\right]\left[1 + 0.1\left(\frac{g}{g_c}\right)\left(\frac{\rho_L - \rho_G}{\tau_w}\right)D_h\right]^{-1/2}, \quad [3]$$

where

D_h = hydraulic diameter (length),
σ = surface tension (force/length)

and

τ_w = wall shear stress (force/area).

Note that at high mass fluxes, the second term of [3] approaches unity.

The quantity ψ may be considered as representing the fraction of the turbulent velocity fluctuations which are capable of penetrating the bubbly layer in the face of the outward flow of vapor from the wall. It is determined from

$$\psi = \frac{1}{\sqrt{2\pi}}\exp\left[-\frac{1}{2}\left(\frac{v_{11}}{\sigma_{v'}}\right)^2\right] - \frac{1}{2}\left(\frac{v_{11}}{\sigma_{v'}}\right)\mathrm{erfc}\left(\frac{v_{11}}{\sqrt{2}\sigma_{v'}}\right), \quad [4]$$

where

G = mass flux (mass/area),
$\sigma_{v'}$ = standard deviation of v'

and

$v' = (G/\rho_L)i_b$.

The evaluation of ψ requires a determination of v_{11}, the average velocity of the vapor flowing out of the bubbly layer. This is computed from

$$v_{11} = \frac{q''_b}{(\rho_G h_{LG})}, \quad [5]$$

where

h_{LG} = enthalpy change on vaporization (energy/mass).

The boiling heat flux, q''_b, required by [5] is obtained from a mass balance on the bubbly layer

$$\frac{q''_b}{h_{LG}} = \psi i_b G(x_2 - x_1), \quad [6]$$

where

x_2, x_1 = qualities of the bubbly layer and core, respectively.

By dividing [6] by [1], the fraction of the total heat flux producing boiling, F, is obtained as

$$F = \frac{q''_b}{q''} = \frac{h_{LG}(x_2 - x_1)}{(h_2 - h_1)}. \quad [7]$$

The CHF is taken as occurring when the void fraction in the bubbly layer, ϵ_2, reaches 0.82. This value was estimated by Weisman & Pei (1983) as the maximum void fraction possible with individual bubbles in the form of slightly flattened ellipsoids. When this void fraction is reached, the bubbles are assumed to agglomerate and form the vapor film leading to CHF. To obtain the value of the CHF, [1]–[6] are solved iteratively until convergence is obtained. In so doing, the bubbly layer quality, x_2, is obtained assuming that the liquid is at the saturation enthalpy. Further, ε_2 and x_2 are related by the homogeneous assumption at high liquid velocities ($V \geqslant 1.6$ m/s) but an allowance for the relative motion of the bubbles is made at lower liquid velocities.

Weisman & Illeslamlou (1988) showed that their revised CHF computation applied with good accuracy to round tube data for water, refrigerant 113 and liquid nitrogen at exit qualities between -0.46 and -0.12. Previous studies by Weisman and coworkers (Weisman & Pei 1983; Ying & Weisman 1986) had shown that the original theory also applied to anhydrous ammonia, liquid helium and refrigerant 11. The experimental data correlated by all three previous investigations (original and revised theory) covered the following broad range:

$$0.012 \geqslant \left(\frac{\rho_G}{\rho_L}\right) \leqslant 0.41,$$

$$V_{SL} > 0.5 \text{ m/s}, \quad G \leqslant 49 \times 10^6 \text{ kg/m}^2 \text{ h}$$

$$0.35 \leqslant L \leqslant 360 \text{ cm},$$

$$0.115 \leqslant D \leqslant 3.75 \text{ cm},$$

$$\varepsilon_{CHF} \leqslant 0.8.$$

Subsequently, Weisman (1988) pointed out that CHF data for water at ~ 0.8 MPa where $\rho_G/\rho_L \simeq 0.005$, could also be correlated by this approach.

3. EXPERIMENTAL STUDIES WITH REFRIGERANT 113

If the revised Pei–Weisman CHF model is valid, it would be expected that the governing heat transfer mechanism (i.e. turbulent interchange at the bubbly layer) should also apply at heat fluxes somewhat below the critical. However, at the outset of this study there did not appear to be suitable boiling curve data which could be compared to an extension of the revised Pei–Weisman theory.

The early subcooled boiling studies of water flowing in a round tube by Kreith & Summerfield (1949) contained only a few points at pressures within the range of the present model and these points were at low heat fluxes. The boiling water data of Clark & Rohsenhow (1952) were taken

at 13.8 MPa (138 bar), where the boiling heat flux changes so rapidly with small changes in wall temperature that the effect of subcooling cannot be easily observed. The more recent subcooled boiling data of Bergles & Rohsenhow (1964), Hino & Ueda (1985) and Muller-Steinhagen *et al.* (1986) were all taken in annuli where the applicability of the equation used by the present approach to evaluate turbulent intensity is doubtful. The data of Del Valle & Kenning (1985) were obtained in a rectangular channel and at pressures below the applicability of the present model. In view of the foregoing, it was decided to obtain new subcooled boiling data which could be compared to the present model. The experiment was also designed to obtain CHF data to provide assurance that the experimental apparatus was yielding data which were consistent with previous observations.

(a) Experimental apparatus

The experimental program was conducted using the University of Cincinnati's boiling refrigerant loop. In this loop, refrigerant 113 is circulated by a pump with a special leakproof seal. Electric heaters allow the freon to be raised to any desired temperature or quality and a water-cooled heat exchanger removes the heat added. The desired pressure is maintained by a bladder-type accumulator which keeps the pressurizing gas away from the refrigerant. Additional details on the loop design have been provided by Crawford *et al.* (1985).

The test sections previously used for two-phase-flow studies were blanked off and a return loop of half inch nominal piping was installed. The heat transfer test section was placed in the central region of this return loop.

The heat transfer test section consisted of a 41 cm length of Inconnel 600 tubing which originally had an o.d. of 0.95 cm ($\frac{3}{8}''$) and an i.d. of 0.62 cm. The central 29 cm of the first test section had its outer diameter machined down to 0.72 cm, giving a wall thickness of 0.051 cm. The tube was welded to an Inconnel 600 flange at both ends. The flanges were insulated from the remainder of the loop by Teflon gaskets and nut washers.

A second test section, which was designed primarily to determine the effect of axially non-uniform heat flux on the CHF, was also used to obtain some of the boiling curve data. This test section was machined from the same length of Inconnel tubing as the axially uniform section and therefore had an i.d. of 0.62 cm. The external diameter was varied so as to produce the lower two-thirds of a cosinusoidally varying heat flux. In the 36 cm machined section, the wall thickness varied from 0.165 to 0.051 cm. Boiling curve data were taken at 36.1 cm from the inlet to the machined section, where the wall thickness was 0.061 cm.

The test sections were heated by direct passage of low voltage a.c. current. The current-carrying cables were attached to Inconnel tabs which are an integral part of the Inconnel flanges. The electrical supply system consisted of a 5 kVA variable autotransformer connected to a single-phase 220 V line. The variable autotransformer output was supplied to a fixed transformer which had a 24 V output and a maximum current-rating of 210 A when fed with 220 V input. Thus, by varying the autotransformer setting, the test section could be supplied a.c. current between 0 and 24 V. The power supplied to the test section was measured by an accurate watt meter which provided a voltage signal as output.

Two stainless-steel sheathed iron–constantan thermocouples were silver soldered to the outside of the machined portion of the uniform test section. One couple was 2.54 cm from the upper end of the machined region while the other was 0.64 cm from the top. To make certain that the thermocouples responded quickly, and also accurately recorded the test section temperature, the junctions were uninsulated. The axially non-uniform test section had five stainless sheathed iron–constantan thermocouples silver soldered to the machined section at 27.0, 30.0, 36.1 and 39.1 cm from the inlet. As noted previously, the boiling curve data taken with this test section was taken with the thermocouple at the 36.1 cm level.

An additional thermocouple was placed on the unheated line below the lower insulated flange and another couple was placed on the unheated line above the upper flange. These couples provided inlet and outlet fluid temperatures.

Signal conditioners removed the a.c. portion of the signals of the test-section couples and amplified the d.c. output of all couples so that they could be read easily on a digital voltameter. A switching circuit allowed any of the couples or the power signal to be read.

The thermocouple and power signals were simultaneously fed to a data acquisition system and a control system. The control system detected the approach of the CHF and protected the installation. When the test-section thermocouples indicated a temperature above a fixed set point, the test-section power was automatically shut off. The power shutoff activated the data acquisition system printer and the last 50 data scans in the system memory were printed.

Loop flow was determined by an orifice placed between flanges in a section of calibrated loop piping. The orifice output was determined by a differential pressure cell which was read visually. Since this signal could not be recorded by the data acquisition system, there remained the possibility that the flow could change during the scan of the thermocouples. Flow and coolant inlet and outlet temperature readings taken before and after the scan showed the flow to be steady during all of the boiling curve runs. However, during some CHF tests variation of the coolant temperature readings indicated the possibility of unstable behavior. In all cases where there was any signficant changes in the coolant temperature thermocouples, the CHF data were rejected.

To make certain that the relationship between signal voltage and temperature was correct, the refrigerant was heated with the loop heater (no current to test section) until a two-phase mixture was obtained and the test-section thermocouples showed a constant output with increasing loop power level. The temperature reading was then compared to the known boiling point at the operating pressure. Good agreement was obtained when a small correction was included to account for the thermocouple fin effect.

Tests were conducted at 0.79 MPa (100 psig) and 0.515 MPa (60 psig). These pressure levels were chosen since they were within the capabilities of the circulating loop yet sufficiently high so that substantial inlet subcooling could be obtained. Boiling curves and CHF values were determined as a function of coolant mass flux and inlet subcooling. Mass fluxes ranged from approx. 2.5×10^6 to 14×10^6 kg/m^2 h and inlet subcooling from 88 to 29° C.

(b) Experimental results

To be certain that the present tests were yielding results which were consistent with previous studies, a series of CHF experiments were first carried out. The tests were conducted with the tube having a uniform thickness over its entire central region. As expected, the critical heat flux occurred at the upper end of the thin-walled section.

Figure 1 compares the data obtained with the predictions from the revised theory of Weisman & Illeslamlou (1988). Since it has been shown that the original Pei–Weisman approach applies to equilibrium qualities > -0.1, the data shown in figure 1 all have qualities (at test-section exit) < -0.1.

It may be seen from figure 1 that generally good agreement between the predictions and measurements is obtained. As suggested by Weisman & Pei (1983), the accuracy of the results is quantified by using the ratio "R", which is defined as

$$R = \frac{\text{Predicted CHF}}{\text{Measured CHF}}. \qquad [8]$$

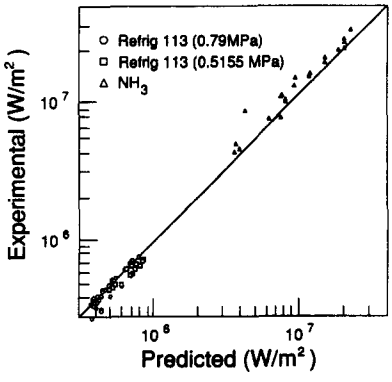

Figure 1. Predicted and experimental CHF values for refrigerant 113 and anhydrous ammonia.

It is found that for the refrigerant 113 data of figure 1 that

$$\mu(R) = 1.03 \quad \text{and} \quad \sigma(R) = 0.089.$$

This indicates that the present tests yielded results which are in agreement with those previously analyzed.

Also shown in figure 1 are the CHF data for highly subcooled ammonia obtained by Bartz (1956) and reported by Bernath (1960). These data were not considered by Weisman & Illeslamlou (1988). In developing Pei & Weisman's (1983) original paper, the slightly subcooled portion of these ammonia data has been predicted. However, the original model was unable to handle data well when $x_e \leqslant 0.15$. However, the present approach is capable of predicting these data even though x_e was as low as -0.3.

Before undertaking subcooled boiling curve measurements, the saturated boiling curves at 7.9 and 5.15 bar were determined. This was accomplished by running the system with nearly saturated liquid entering the heated test section. Only those points which were clearly in the quality region at the measurement location were accepted. However, exit qualities were all quite low and all points were far below the condition at which boiling suppression factors apply. The results of these tests are plotted in figure 2. While there is some scatter, a single curve results for each pressure. The mass flux does not appear to have a significant effect in the fully developed saturated boiling region. This is in accord with the observations of previous investigators such as Kenning & Cooper (1989), Thom *et al.* (1965/66), Bergles & Rohsenow (1964) and Jens & Lottes (1951).

Subcooled boiling curves were determined for a series of fixed inlet temperatures and velocities for both 0.515 and 0.79 MPa. Figure 3 compared the subcooled data, obtained at a fixed mass flux of 9.8×10^6 kg/m^2 h at 0.515 MPa for three different inlet subcoolings, to the saturated boiling curve. At the lowest heat fluxes, we see the relationship between heat flux and wall temperature expected in forced convection. At wall temperatures above saturation (106°C), the heat flux sharply increases. Note that hysteresis is observed in some cases with the wall temperature actually

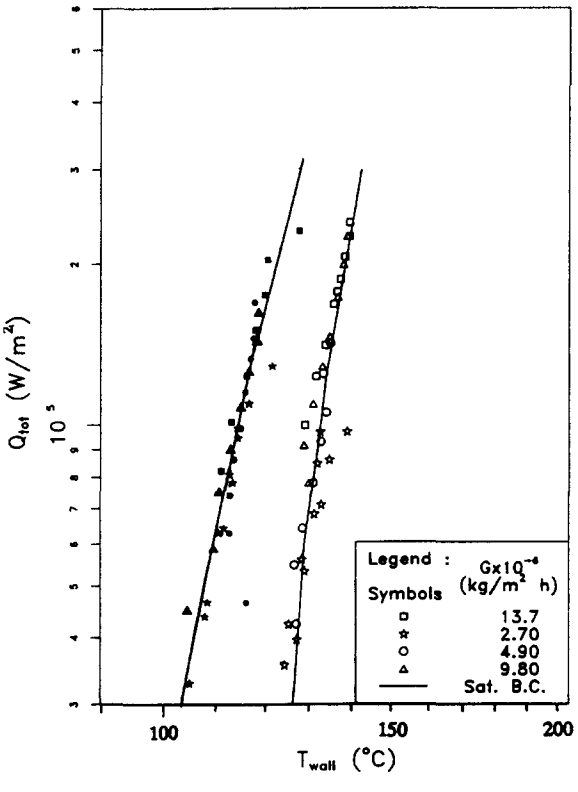

Figure 2. experimentally determined saturated boiling curves for refrigerant 113 [$P = 0.79$ MPa (open symbols, $P = 0.515$ MPa (solid symbols)].

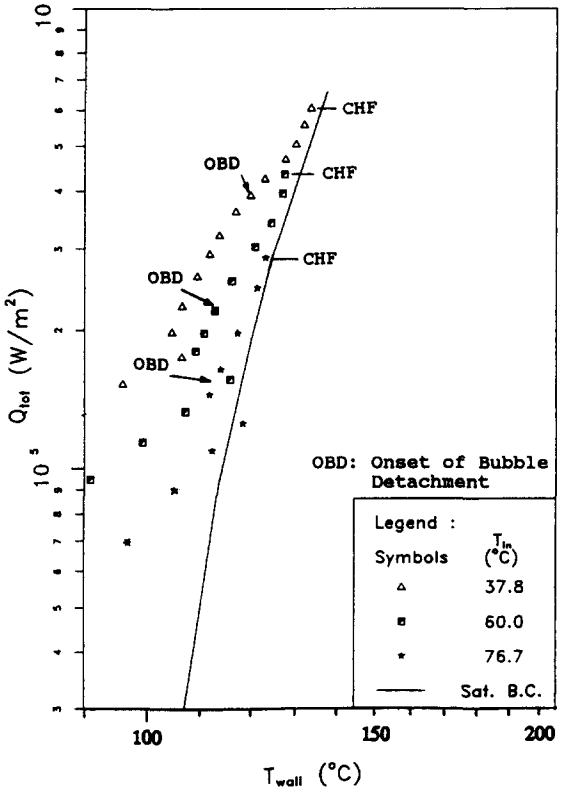

Figure 3. Effect of coolant inlet temperature on subcooled boiling curves ($P = 0.515$ MPa, $G = 0.8 \times 10^6$ (kg/m^2 h), refrigerant 113).

falling once boiling begins. Further increases in heat flux cause the wall temperature to rise as expected.

In order to mark the detached bubble region in which a modified Pei–Weisman model may apply, each curve has an arrow showing the onset of bubble detachment (OBD). All data points to the right of the OBD arrow are in the detached region. The bubble detachment point was determined using the method of Levy (1967), as recommended by Weisman & Pei (1983).

For the tests shown in figure 3, inlet subcooling ranged from a maximum of 68.5°C to a minimum of 29.6°C. With such substantial subcooling, the bulk fluid was subcooled up until the upper limit of the curve at the CHF (denoted by arrow and CHF). At the CHF flux and location, the local thermodynamic quality, defined as $(h_l - h_f)/h_{LG}$, ranged from -0.23 to -0.08.

The observed subcooled boiling curves all lie above the saturated boiling curve. As expected, the distance between the saturated and subcooled boiling curves is greatest for the highest inlet subcooling. At the high heat fluxes where the subcoolings have been reduced, the saturated and subcooled boiling curves approach each other.

Figure 4 compares the saturated boiling curve with subcooled boiling data taken at 0.79 MPa with an inlet subcooling of 77°C and a series of mass fluxes. It will be noted that at this pressure there is no boiling curve hysteresis. Further, in contrast to the saturated boiling situation, increasing mass flux brings about a significant increase in the observed heat transfer rate at a given wall temperature. At the highest mass flux, the subcooled boiling curve remains significantly above the saturated boiling curve even at the CHF point.

It is clear from the foregoing, that any model of boiling in the detached region must show the following trends:

(a) Increased rates of heat transfer with increased subcooling.
(b) Increased rates of heat transfer with increased mass flux.
(c) Approach the saturated boiling curve as the subcooling approaches zero.

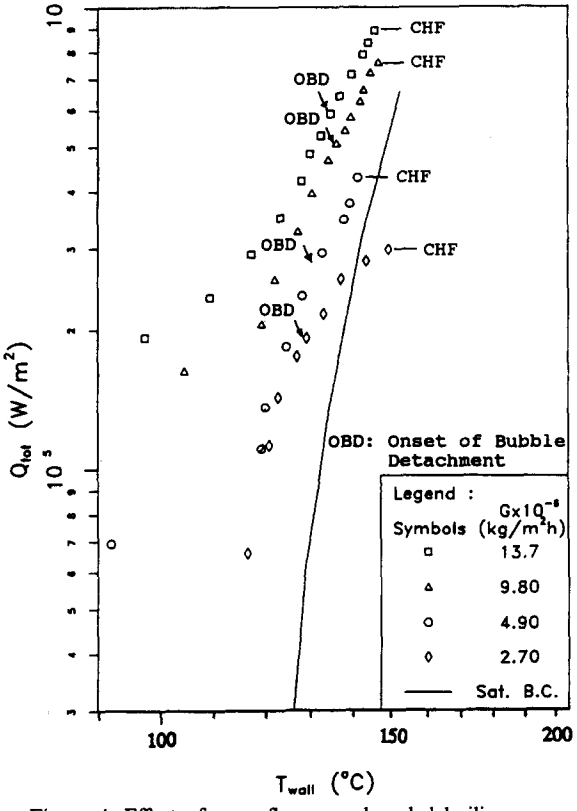

Figure 4. Effect of mass flux on subcooled boiling curves ($P = 0.79$ MPa, $T_{in} = 48.9$°C, refrigerant 113).

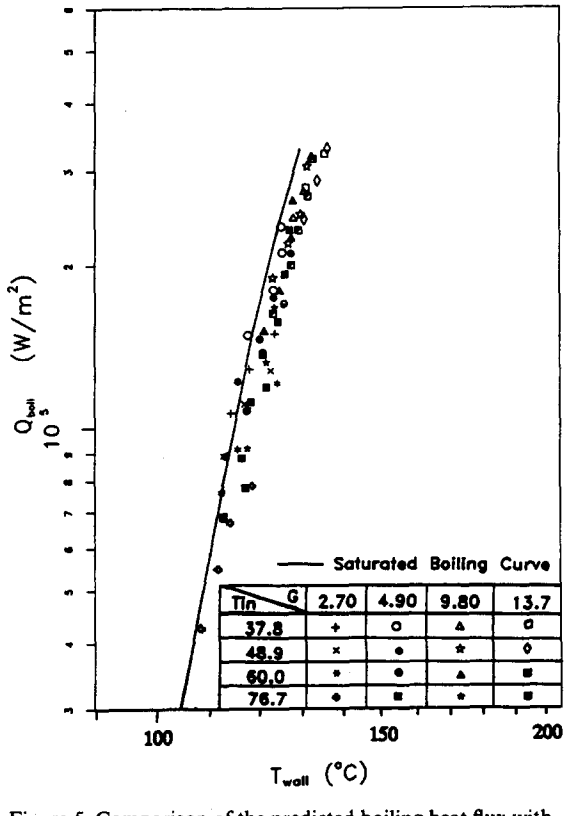

Figure 5. Comparison of the predicted boiling heat flux with the saturated boiling curve ($P = 0.515$ MPa, refrigerant 113).

4. EXTENSION OF THE TURBULENT INTERCHANGE MODEL TO HEAT FLUXES BELOW THE CHF

If turbulent interchange at the edge of the bubbly layer really governs the heat transfer at the CHF, it should also govern the heat transfer rate at somewhat lower heat fluxes. The extension of the turbulent interchange approach is based on the following assumptions:

(a) Turbulent interchange at the edge of the bubbly layer governs the rate of heat transfer throughout the detached region.
(b) For a given fluid–surface combination at a fixed pressure and gravitational acceleration, there is a unique relationship between heater surface temperature and boiling heat flux.

The turbulent interchange at the bubbly layer edge is still governed by the mass and energy balances written previously, [1] and [6]. However, as the void fraction in the bubbly layer is reduced, the effect of the bubbles on the turbulent intensity should be reduced. At very low bubbly layer void fractions, the turbulent intensity should approach the single-phase value. It was therefore assumed that the $(\rho_L - \rho_G)/\rho_G$ multiplier in the equation providing the turbulent intensity corresponded to the value which applies when $\varepsilon_2 = 0.82$; the bubbly layer void fraction at CHF. For simplicity, it was further assumed that this effect varied with $[\varepsilon_2^n]$, where "n" is an empirical parameter to be determined; i.e.

$$i_b = 0.46(K)^{0.6}\,\mathrm{Re}^{-0.1}\left(\frac{D_b}{D}\right)^{0.6}\left[1 + \left(\frac{\varepsilon_2}{0.82}\right)^n a\frac{(\rho_L - \rho_G)}{\rho_G}\right] \qquad [9]$$

and ε_2 = volume fraction of vapor in the bubbly layer. Once a value for "n" has been determined, an iterative solution for ε_2 is available. An arbitrary assumption of ε_2 leads to a value of i_b which then allows computation of h_2, the enthalpy of the bubbly layer fluid. With the assumption that the liquid in the bubbly layer is at the saturation enthalpy, h_f, an improved x_2 and ε_2 may be obtained. The computation continues until the assumed and calculated ε_2 agree.

The bubbly layer enthalpy, h_2, obtained by the foregoing computation allows the boiling heat flux, q_b'', to be obtained via [7]. With the assumption that the relationship between wall temperature and boiling heat flux is unique for a given system at a given pressure, the wall temperature is then obtained from the saturated boiling curve.

To determine the most appropriate value of the void fraction exponent to be used in [8], computations were made for a series of "n" values. At each n value, using the foregoing calculation procedure, the boiling heat flux was determined for the experimental points in the detached region. However, instead of obtaining the wall temperature from the saturated boiling curve, the calculated boiling heat flux was plotted against the experimentally observed wall temperature. If the suggested approach is valid, then all of the experimental observations at a given pressure should cluster along the saturated boiling curve.

Best results were obtained for all the data with "n" set at 2.5. The results obtained with this value of "n" are shown for 0.515 MPa in figure 5. Excluded from this plot were those points just below the CHF, since there was some indication that many of these points were actually in the transition boiling region. It may be seen that generally good results are obtained with the points at the various mass fluxes and subcoolings being brought together. However, there is a tendency for the predicted boiling heat flux to fall below that expected. Similar results were obtained at 0.79 MPa.

The degree of agreement of the total predicted heat flux in the detached region and total observed flux is more readily seen in figures 6–9. The points plotted show the total heat flux and inner wall temperature derived from the experimental observations. For the detached region, curves showing the predicted variation of wall temperature with total heat flux are also shown. These curves were obtained by assuming a total heat flux, computing a corresponding boiling heat flux and then obtaining a wall temperature from the appropriate saturated boiling curve. In addition, the Dittus–Boelter forced convection equation is shown for the forced convection region at low heat fluxes.

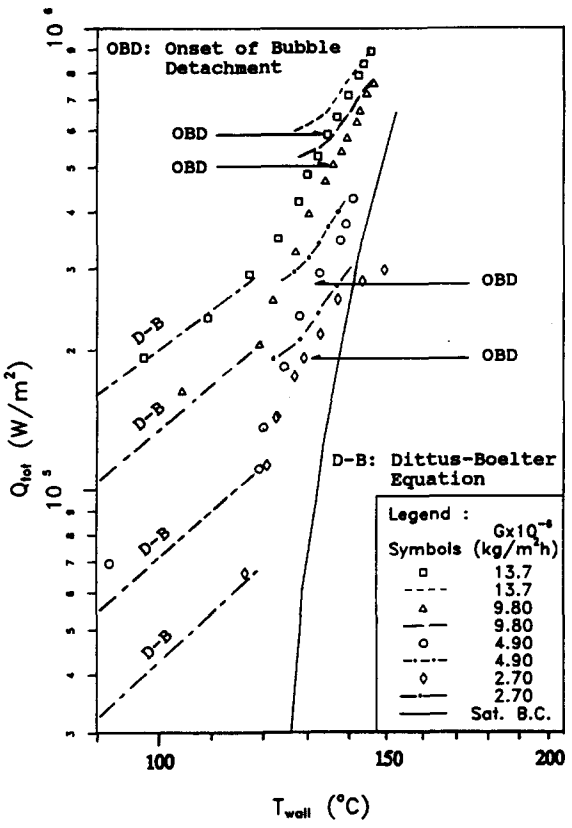

Figure 6. Comparison of the predicted subcooled boiling curve with experimental observations ($P = 0.79$ MPa, $T_{in} = 48.9$°C, refrigerant 113)—influence of mass flux.

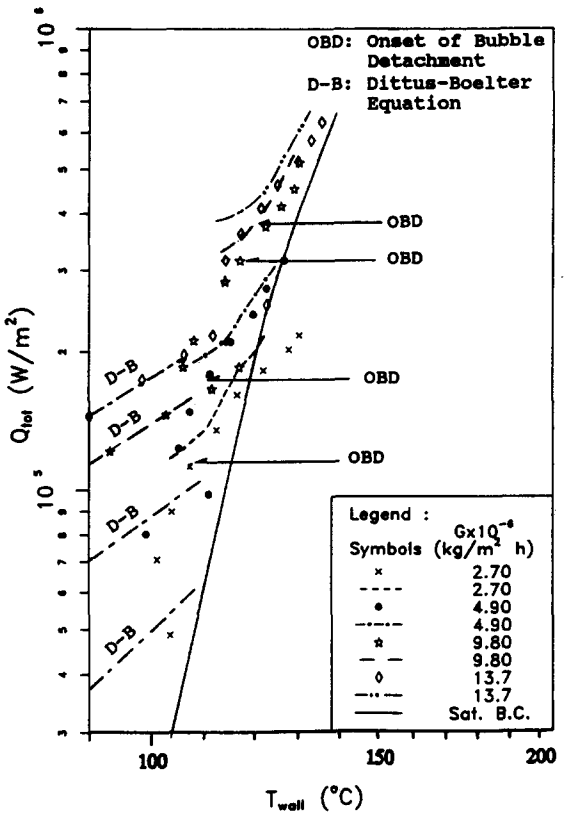

Figure 7. Comparison of the predicted subcooled boiling curve with experimental observations ($P = 0.515$ MPa, $T_{in} = 48.9$°C, refrigerant 113)—influence of velocity.

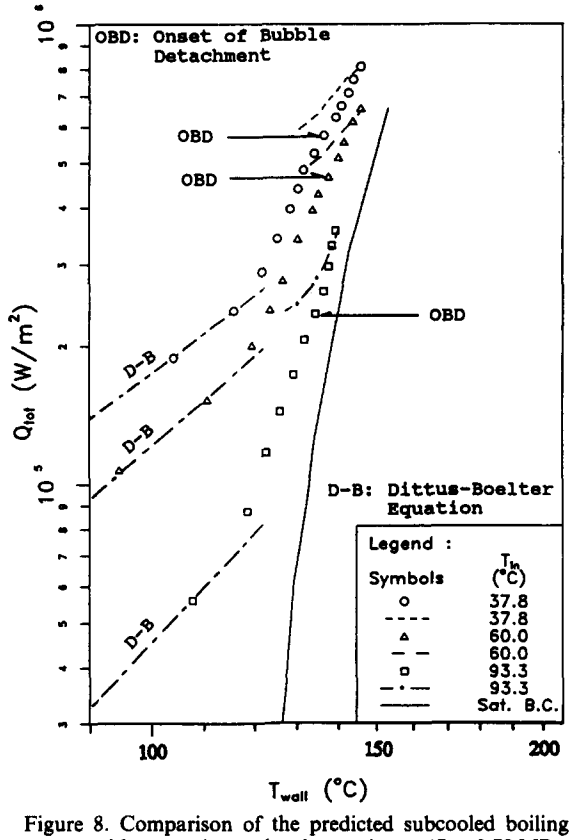

Figure 8. Comparison of the predicted subcooled boiling curve with experimental observations ($P = 0.79$ MPa, $G = 9.8 \times 10^6$ kg/m^2 h, refrigerant 113)—influence of inlet temperature.

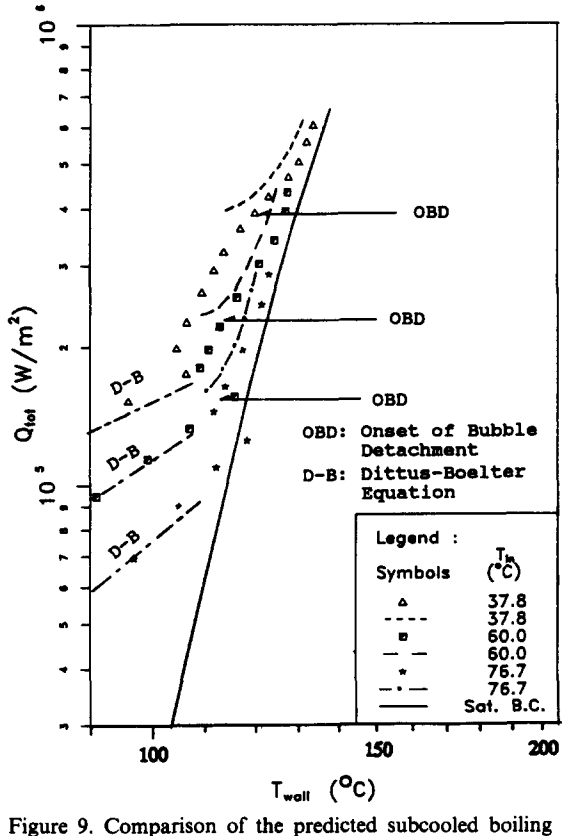

Figure 9. Comparison of the predicted subcooled boiling curve with experimental observations ($P = 0.515$ MPa, $G = 9.8 \times 10^6$ kg/m^2 h, refrigerant 113)—influence of inlet temperature.

Figures 6 and 7 illustrate the effect of mass flux on the subcooled boiling curves at 0.515 and 0.79 MPa with the inlet temperature held at 49°C. It is seen that the trend of increased total heat flux at increased mass flux is correctly predicted. There is some tendency for the data to show higher wall temperatures (greater boiling flux) at a given total flux than the predictions. However, at the higher heat fluxes predicted and observed heat fluxes are within 20% of each other. As the onset of the detached region is approached, the discrepancy between predictions and observations increases.

Figures 8 and 9 show the effect of inlet subcooling on the subcooled boiling curves at 0.515 and 0.79 MPa with the mass flux held at 9.8×10^6 kg/m^2 h. It may be observed that the predictions correctly show the effect of increased subcooling in increasing the total heat flux. As in the two previous figures, agreement between predictions and observations are generally within 20% at the high heat fluxes but significant discrepancies arise as the onset of the detached bubble region is approached.

The discrepancies between predictions and observations near the OBD are readily explained. In evaluation of the boiling fraction via [7], we rely on the quality of the bubbly layer, x_2. The value of x_2 is obtained from the bubbly layer enthalpy, h_2, obtained from [1] and the assumption that the fluid in the bubbly layer is at thermodynamic equilibrium. At heat flux values close to the bubble detachment point, values of h_2 which are only very slightly above h_f, the enthalpy of the saturated liquid, are calculated. We therefore obtain x_2 and boiling fraction values close to zero. This is clearly not the case as there is a significant boiling heat flux in the attached region. The assumption of thermodynamic equilibrium at the bubbly layer edge thus appears to be incorrect in the region of the bubble detachment point. When heat fluxes are 20–25% above this value, it appears that the thermodynamic equilibrium assumption is appropriate since reasonable boiling curve predictions are obtained.

If the proposed approach is valid at all levels of subcooling, it should also apply with slightly subcooled liquid where the predictions should approach the saturated boiling curve. This question is examined in figure 10 where experimentally derived observations are compared to model predictions in the detached region for liquid which enters with only 16°C subcooling. As may be seen, the experimental data and predicted curve are in good agreement. They both approach the saturated boiling curve as h_1, the bulk fluid, enthalpy approaches h_f. Weisman & Illeslamlou (1988) have previously shown that F, the boiling fraction, equals unity when $h_2 \geqslant h_f$. The predictions thus will lie along the saturated boiling curve once saturation is reached and no mass velocity influence will be shown. This is in accord with the experimental evidence.

It appears that the present model of subcooled boiling in the detached bubble region provides reasonable boiling curve predictions for most of the detached region. Reasonable predictions are obtained so long as the heat flux is sufficiently above the detachment point so that the assumption of thermodynamic equilibrium in the bubbly layer is appropriate.

5. ONSET OF THE DETACHED BUBBLE REGION

It seems reasonable to postulate that the onset of the detached bubble region corresponds to the location at which h_2, the bubbly layer enthalpy, equals h_f, the enthalpy of saturated liquid. Although the absence of thermodynamic equilibrium at this point indicates the possibility of some voids in the bubbly layer region when $h_2 \leqslant h_f$, one would not expect any significant growth of voids in the core region until the fluid entering the core from the bubbly layer has an enthlpy above h_f. We therefore rewrite [1] at the onset of the detached region as:

$$q'' = G\psi i_b(h_f - h_{ld}) \qquad [10]$$

where h_{ld} represents the bulk fluid enthalpy at the point of bubble departure.

Although experimental observations indicate there are a few bubbles which enter the core region just prior to the onset of the detached region, the number is quite low. Hence, the quantity v_{11}, represents the average velocity of the vapor flowing into the core, is close to zero. A close

approximation of ψ can therefore be obtained by the analytical integration of [4] taking v_{l1} as zero. We then have

$$(h_f - h_{ld}) = \sqrt{2\pi}\frac{q''}{i_b G}. \quad [11]$$

Further, since the void fraction in the bubble layer is quite low at the bubble departure point, and since the two-phase multiplier of i_b varies with $(\varepsilon_2)^{2.5}$, the single-phase value of i_b, the turbulent intensity, is a good approximation. Hence,

$$(h_f - h_{ld}) = \frac{\sqrt{2\pi}\left(\frac{q''}{G}\right)}{0.79\,\mathrm{Re}^{-0.1}\left(\frac{D_b}{D}\right)^{0.6}}. \quad [12]$$

The theoretically based criterion of Levy (1967) and the empirically based criterion of Saha & Zuber (1974) are now generally considered the most reliable of the available bubble departure point predictions. When rewritten in the form suggested by Lahey & Moody (1977), the Saha & Zuber (1974) criterion for $\mathrm{Pe} > 70{,}000$ is given by

$$(h_f - h_{ld}) = 154\frac{q''}{G}. \quad [13]$$

The strong similarity between [11] and [13] is evident. However, the present approach shows a tube diameter effect not seen by Saha & Zuber (1974).

To evaluate how the proposed bubble departure criterion compares with those of Saha & Zuber (1974) and Levy (1967). All these criteria were evaluated for refrigerant 113 and water over a range of conditions. Tube diameters of 0.61 and 1.27 cm (0.24″ and 0.50″) were considered at mass fluxes ranging from 2.45×10^6 to $9.8 \times 10^6\,\mathrm{kg/m^2\,h}$. Pressures of 0.515 and 0.79 MPa were used for refrigerant 113 while pressures of 3.45 and 6.9 MPa were used for water. Heat fluxes were varied

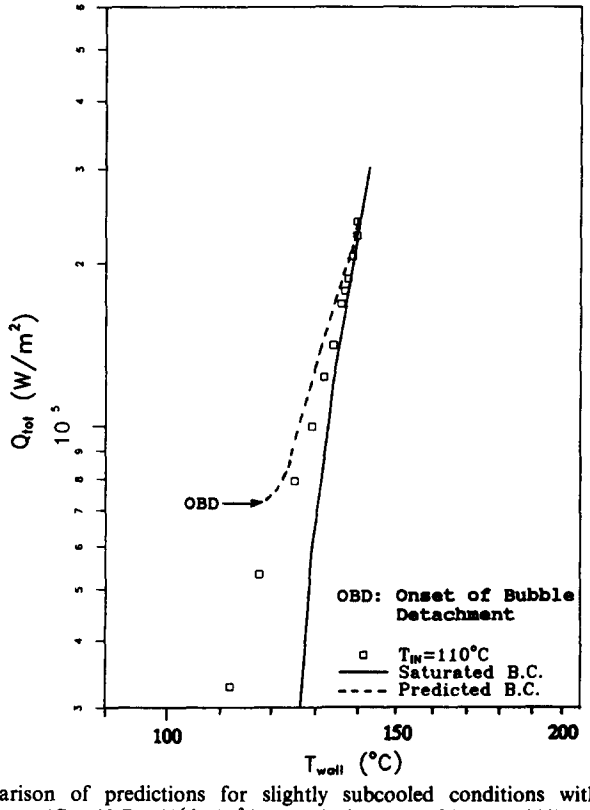

Figure 10. Comparison of predictions for slightly subcooled conditions with experimental data ($G = 13.7 \times 10^6\,\mathrm{kg/m^2\,h}$, $P = 0.79$ MPa, refrigerant 113).

Table 1. Comparison of bubble departure criteria

Fluid	Tube dia (cm)	$\frac{(\Delta h)_I}{(\Delta h)_L}$	$\frac{(\Delta h_I)}{(\Delta h_{S+Z})}$
Refrigerant 113	0.61	1.00	1.27
Refrigerant 113	1.27	0.89	1.19
Water	0.61	1.17	1.22
Water	1.27	1.24	1.12

ΔH_I = Mean value of $(h_f - h_{id})$ computed from [10] for conditions examined.
ΔH_L = Mean value of $(h_f - h_{id})$ computed from Levy (1967) bubble departure criteria for conditions examined.
ΔH_{S+Z} = Mean value of $(h_f - h_{id})$ computed from Saha & Zuber (1974) bubble departure criteria for conditions examined.

over a range appropriate to each fluid. Mean values of the ratios of the departure subcoolings $(h_f - h_{id})$ computed by [10] to those from the Saha & Zuber (1974) and Levy (1967) approaches are shown in table 1. It may be seen that the present predictions for refrigerant 113 tend to lie between those of the Levy (1967) and Saha & Zuber (1974) approaches. For water, however, the subcoolings of [10] are about 20% above those of the Saha & Zuber and Levy computations.

The present approach would appear to provide a phenomenological foundation for the form of the Saha & Zuber (1974) bubble departure criterion. Moderate quantitative agreement is obtained between the onset of the detached region from the present approach and those from the Levy and Saha & Zuber predictions. The tendency of the present approach to require higher subcoolings may be reflective of the lack of thermodynamic equilibrium with, perhaps, the need to use i_b values reflecting the vapor flow from the wall into the bubbly layer at the detachment point.

6. USE OF THE BOILING CURVE PREDICTION IN CHF COMPUTATION AT HIGH PRESSURE AND HIGH MASS FLUXES

Yagov & Puzin (1985) have observed that, at high CHF obtained at high mass velocities and high pressures, there were a number of CHF points which were not determined by their usual CHF correlation but were limited by a maximum wall temperature. For their high-pressure water data, they concluded that this maximum temperature, or thermodynamically limiting temperature, was given by a modification of the method of Skirpov (1972), where the limiting pressure, p_L, is given by

$$p_s - p_L = 1.32\sigma^{3/2}(kT_s)^{-1/2}, \quad [14]$$

where

k = Boltzman constant,
P_s = saturation pressure (force/area)

and

T_s = saturation temperature (K).

The curve of p_L vs T_s so obtained defines the so-called thermodynamically limiting temperature for any given pressure.

While Yagov & Puzin (1985) were able to match their experimental data with observed wall temperatures to [14], they did not suggest a method by which the wall temperature could be calculated under subcooled boiling conditions in the approach.

For a given heat flux, [1]–[5] and [7] are used to compute the boiling heat flux. The boiling heat flux together with a known saturated boiling curve allows calculation of the heater wall temperature. If this temperature equals or exceeds the so-called thermodynamically limiting temperature, then CHF has been reached or exceeded even though [1], with h_2 set at a value corresponding to $\varepsilon_2 = 0.82$, does not predict CHF.

7. BOILING CURVE PREDICTIONS IN THE ATTACHED REGION

Although somewhat beyond the original scope of this investigation, the subcooled boiling curves in the attached region were examined. The most popular method for predicting the total heat flux in this region is the superposition method of Rohsenhow (1952). In this approach, the total heat flux is taken as the sum of the boiling heat flux and the heat transferred to the liquid by single-phase forced convection; i.e. the total heat flux, q''_t, is given by

$$q''_t = q''_b + q''_{conv} \quad [15]$$

where

$q''_{conv} = h'(T_w - T_L)$.
h' = single-phase convective heat transfer coefficient (energy/area time)

and

T_L, T_w = liquid and wall temperatures, respectively.

The adequacy of this approach was tested by subtracting the calculated single-phase forced convection heat flux from the observed total flux and plotting the resultant q''_b against observed wall temperature. For consistency, the results were compared against a saturated boiling curve obtained by subtracting the calculated force convection flux from the observed total flux. Typical results are shown in figure 11.

It may be seen that although those data points at a low subcooling (points a high flux and high inlet temperature) lie close to the revised saturated boiling curve, the more highly subcooled points

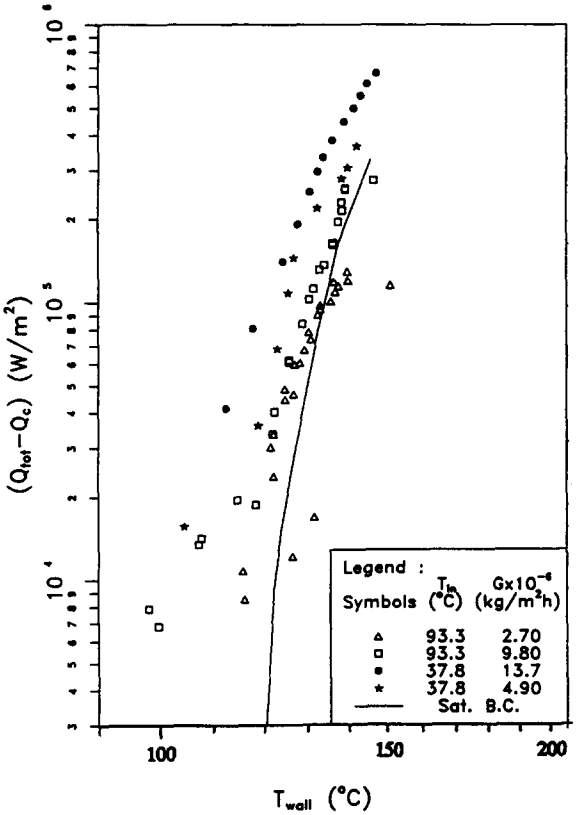

Figure 11. Comparison of the calculated boiling curve with the saturated boiling curve using Rohsenow's (1952) superposition approach ($P = 0.79$ MPa, refrigerant 113). *Note*: the saturated boiling curve was obtained by subtracting the convective heat transfer component from the total.

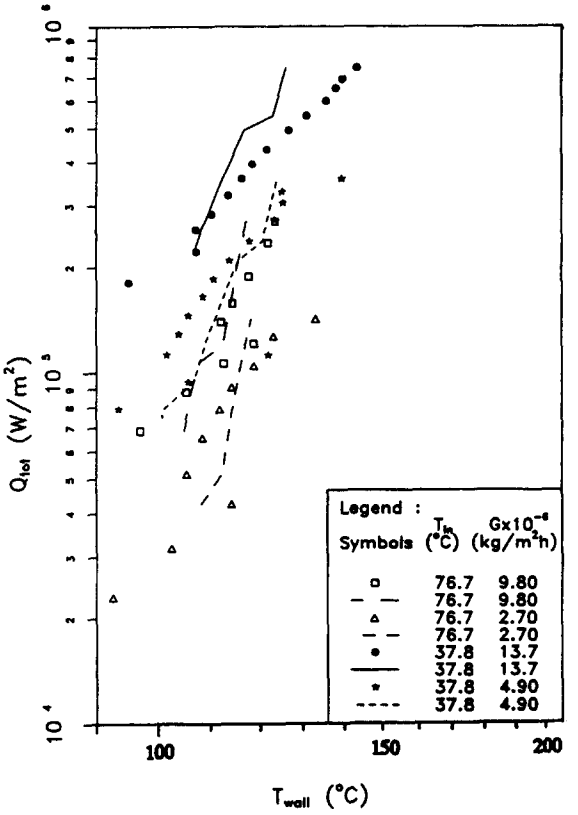

Figure 12. Comparison of the subcooled boiling data with Shah's (1977) correlation ($P = 0.515$ MPa, refrigerant 113).

lie above the revised saturated boiling curve. The greater the subcooling, the greater the deviation from the saturated boiling curve. The present results are similar to the observations of Del Valle & Kenning (1985). These results indicate that the convective component of the total heat transfer is underestimated by taking it as equal to the single-phase value.

More recently, subcooled boiling correlations have been proposed by Bjorge *et al.* (1982), Shah (1977) and Kandlikar (1989). Bjorge *et al.* (1982) used a modified superposition scheme. They proposed

$$q''_t = [q''^2_{conv} + (q''_b - q''_{in})^2]^{1/2}, \quad [16]$$

where

q''_{in} = heat flux required to initiate boiling

and other symbols have their previous meaning. Use of [16] yields lower values of q''_t than the simple superposition procedure of Rohsenhow (1952). Since the Rohsenhow approach itself falls below the experimental observations, even greater disagreement is seen when the data is compared to [16].

Shah's (1977) approach is somewhat more complex. He proposed a correlation having a product form where

$$q''_t = h'_c \Phi (T_w - T_s); \quad [17]$$

if $(T_s - T_b)/(T_w - T_s) > 2$ or $630000\text{Bo}^{1.25}$,

$$\Phi = \Phi_0 + (T_w - T_b)/(T_w - T_s);$$

otherwise

$$\Phi = \Phi_0;$$

and

$$\Phi_0 = 230\text{Bo}^{0.5} \quad \text{for Bo} \geqslant 3 \times 10^{-5},$$
$$\Phi_0 = 1 + 46\text{Bo}^{0.5} \quad \text{for Bo} < 3 \times 10^{-5},$$
$$\text{Bo} = q''_t/(Gh_{LG}).$$

While Shah's correlation shows the same trends as the experimental data with respect to velocity and subcooling, quantitative agreement is only moderate at best. Typical results are shown in figure 12.

Kandlikar (1989) has proposed a modification of the Shah correlation which revises the predictions at low heat fluxes. Kandlikar suggests the addition of a "partial subcooled boiling" region. In this region, the subcooled boiling curve is described by an equation of the form

$$q''_t = a + b(\Delta T_s)^n. \quad [18]$$

The constants a and b are determined so that (i) one end of the curve is on the forced convection curve at the initiation of boiling and (ii) the other end is on Shah's subcooled boiling curve at a heat flux designated q''_W. This quantity is given by

$$q''_E = 1.4q''_D. \quad [19]$$

The parameter q''_D is the heat flux at the intersection of the forced convection (Dittus–Boelter) curve with Shah's subcooled boiling prediction.

The Kandlikar modification of Shah's prediction does produce somewhat improved agreement at the lowest heat fluxes. It is thus possible to obtain moderate agreement with the present experimental data by using the Shah–Kandlikar approach for the attached bubble region and the model proposed in this paper in the detached bubble region. However, this approach does not generally yield a continuous boiling curve prediction since the present model and the Shah predictions often fail to intersect.

In view of the foregoing and the fact that the deviations from the simple superposition approach were systematic in nature, a revised superposition model was considered. It was observed that

previous investigators, including Bowring (1962), Forster & Grief (1959) and Rouhani & Axelson (1970) among others, noted the need to enhance the convective heat transfer component of [15]. It has generally been assumed that this enhancement is proportional to the boiling heat flux. Equation [15] is therefore rewritten as

$$q''_{\text{total}} = (1 + e)q''_{\text{b}} + q_{\text{conv}}. \quad [20]$$

where e represents the enhancement factor reflecting additional convection (microconvection) due to bubble motion. Bowring (1962) suggested means for computing e for the water–steam system. Based on Forster & Grief's (1959) idea that the vapor leaving the wall region must be replaced by an equal volume of liquid which must be raised to saturation, Rouhani & Axelson (1970) suggested that e be computed from

$$e = \rho_{\text{L}} \frac{h_{\text{f}} - h_{\text{L}}}{\rho_{\text{G}} H_{\text{LG}}}. \quad [21]$$

Values of e computed from [21] were used to recompute the forced convection flux for the boiling curve data obtained in the present tests. It was found that the values of e so obtained overestimated the forced convection component. The overestimation was particularly marked at 0.515 MPa.

It was found that if e was represented by

$$e = 3 \frac{h_{\text{f}} - h_{\text{L}}}{H_{\text{LG}}}, \quad [22]$$

where

$h_{\text{f}} - h_{\text{L}}$ = saturated and liquid enthalpies, respectively,

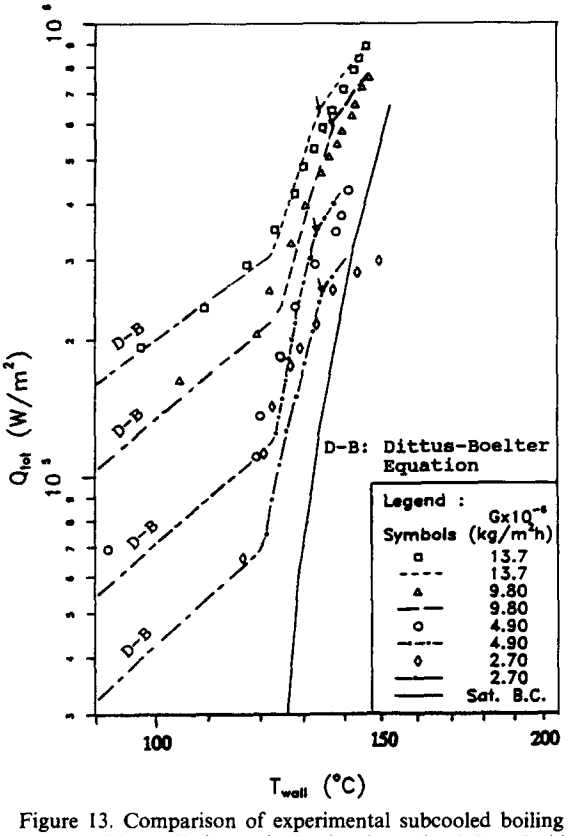

Figure 13. Comparison of experimental subcooled boiling curves with predictions obtained using $q''_{\text{b}} = (q''_{\text{t}} - q''_{\text{conv}})/[1 + 3(h_{\text{f}} - h_{\text{L}})/h_{\text{LG}}]$ in the attached bubble region and the extended Weisman–Pei theory in the detached bubble region ($P = 0.79$ MPa, $T_{\text{in}} = 48.9$°C, refrigerant 113)—effect of velocity.

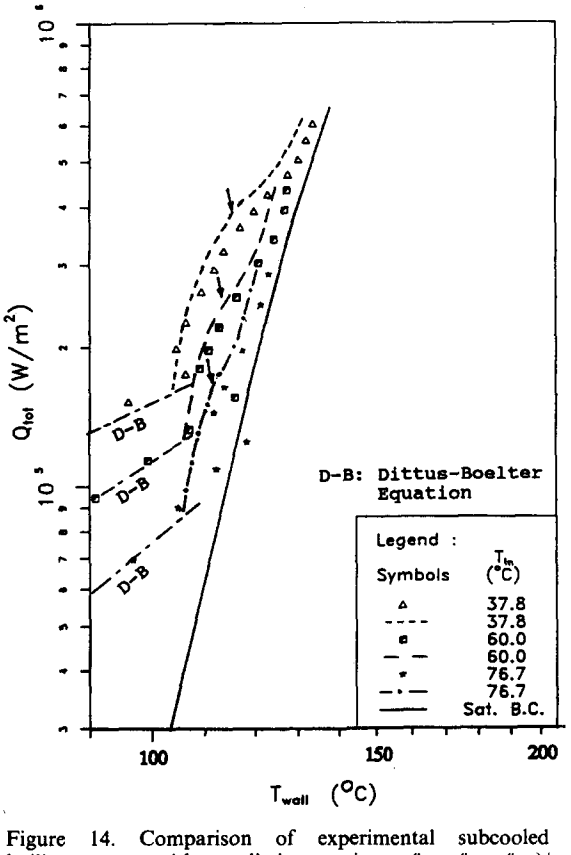

Figure 14. Comparison of experimental subcooled boiling curve with predictions using $q''_{\text{b}} = q''_{\text{t}} - q''_{\text{conv}})/[1 + 3(h_{\text{f}} - h_{\text{L}})/h_{\text{LG}}]$ in the attached bubble region and the extended Weisman–Pei theory in the detached bubble region ($P = 0.515$ MPa, $G = 9.8 \times 10^6$ kg/m^2 h, refrigerant 113)—effect of inlet temperature.

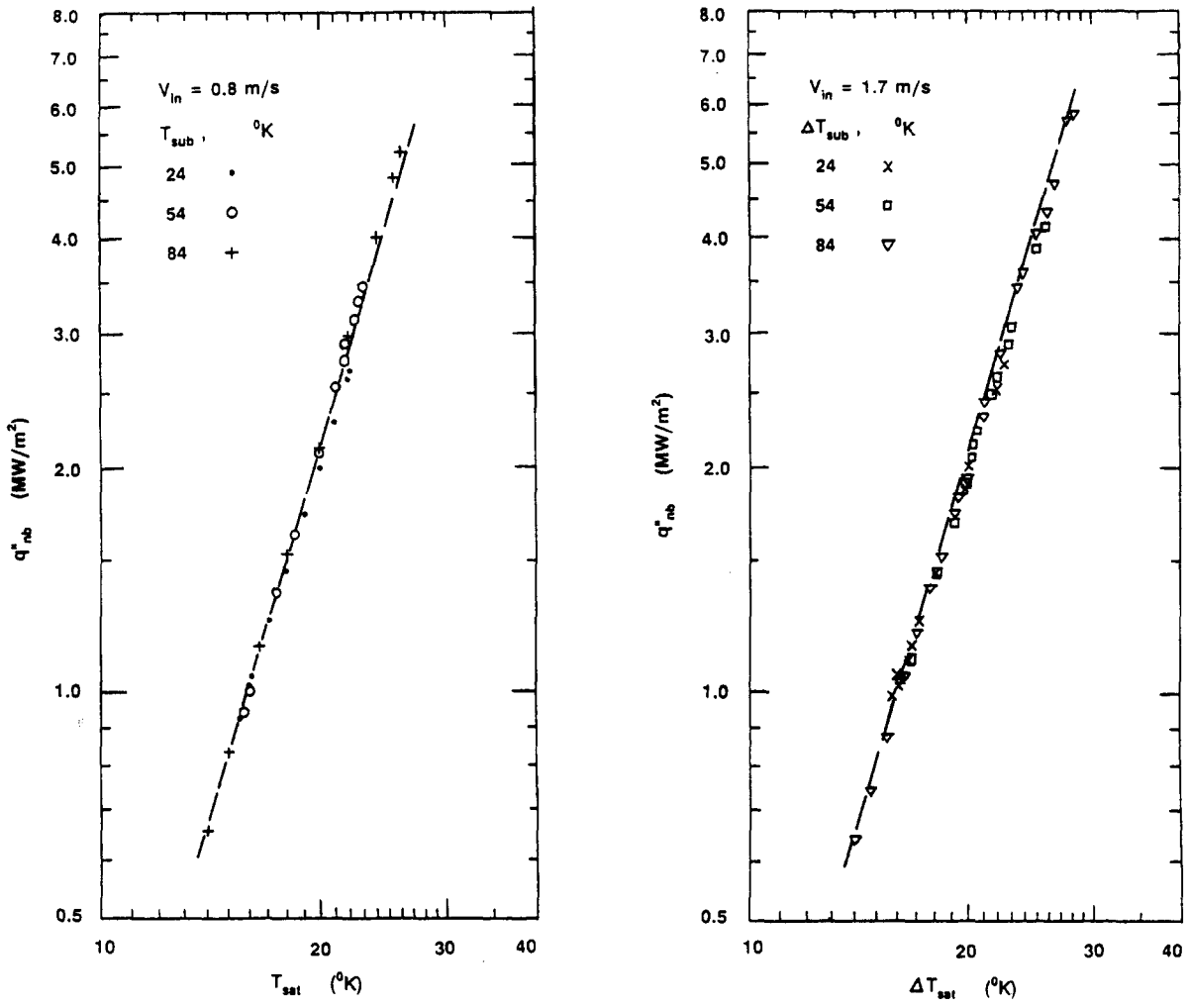

Figure 15. Boiling heat flux predictions in the attached region for water at 0.12 MPa.

the data of the present tests in the attached region could be reasonably represented. Figures 13 and 14 show typical comparisons between this prediction procedure and the experimental data. In these figures, [20] and [22] have been for the attached region predictions and the detached region model for the detached region. As may be seen, generally reasonable agreement was obtained.

To see if [22] might have application to any other systems, it was applied to the low-pressure (approx. 0.1 MPa) data of Kenning & Del Valle (1985) for boiling of water. Only the data for the thickest heater (0.02 cm) was considered. As the vapor–liquid density ratio is outside the range of the detached region model, these data were treated in the same manner as those shown in figure 11; i.e. the boiling heat flux, q''_b was determined as

$$q''_b = q''_{total} - q''_{conv}/(1+e), \qquad [23]$$

with e being computed from [22]. Examination of figure 15 shows that this procedure brings the data at the various subcooling into a single curve. Since the dashed line shown in both figures 15(a) and 15(b) is given by the same equation, it is seen that the resulting boiling curve is, as expected, independent of fluid velocity. Equation [22] would then appear to be useful for both refrigerant 113 and water.

8. CONCLUSION

The present investigation suggests that separate approaches should be used for calculating subcooled boiling heat transfer in the attached and detached bubble regions. In the attached bubble

region, the total heat transfer appears to be the sum of boiling, single-phase convection and microconvection components. A procedure for determining the microconvection component is suggested. Although the microconvection computation procedure works with both refrigerant 113 and low-pressure water, additional data is needed to determine whether it is generally applicable.

In the detached bubble region, the present work strongly suggests that the heat transfer is governed by the turbulent interchange at the edge of the bubbly layer. The bubbly layer interchange model appears to adequately predict the observed trends with respect to subcooling and mass velocity. Further, the bubbly layer interchange model predicts the experimental observations that, as the subcooling goes to zero, the boiling heat transfer approaches the saturated boiling curve. Use of a simple superposition model leads to overprediction of the heat transfer at zero subcooling.

The ability of the bubbly layer interchange model to predict boiling heat transfer at heat fluxes below CHF would appear to add support to the view that interchange at the bubbly layer edge governs subcooled and low quality CHF.

Acknowledgements—This article is based in part on a paper presented at the *Meeting of the American Nuclear Society*, Nov. 1990.

The authors also wish to acknowledge the financial support of the National Science Foundation.

REFERENCES

BARTZ, D. R. 1956 Jet Propulsion Lab. Memo. JLP 20-137- CIT, Pasadena, Calif.

BERGLES, A. & ROHSENHOW, W. M. 1964 The determination of forced convection surface boiling heat transfer. *Trans. ASME. Ser. C.* **86,** 365–372.

BERNATH, L. 1960 A theory of local boiling burnout and its application to existing data. *Chem. Engng Prog. Symp. Ser.* **56**(30), 95–116.

BJORGE, R. W., HALL, G. R. & ROHSENOW, W. M. 1982 Determination of forced convection surface boiling heat transfer. *J. Heat Transfer* **25,** 753–757.

BOWRING, R. W. 1962 Physical model based on bubble detachment and calculation of steam voidage in subcooled region of heated channel. Report HPR-10 OECD Halden Reactor Project.

CLARK, J. A. & ROHSENOW, W. M. 1952 Local boiling heat transfer to data at low Reynolds number and high pressures. *Trans. ASME* **76,** 553.

CRAWFORD, T. J., WEINBERGER, C. B. & WEISMAN, J. 1985 Two-phase flow patterns and void fractions in downward flow. Part I: steady-state flow patterns. *Int. J. Multiphase Flow* **11,** 761–782.

DEL VALLE, V. H. & KENNING, D. B. R. 1985 Subcooled flow boiling at high heat flux. *Int. J. Heat Mass Transfer* **28,** 1907–1920.

FORSTER, K. & GRIEF, R. 1959 Heat transfer to a boiling liquid; mechanism and correlations. *Trans. ASME J. Heat Transfer* **81,** 43–51.

HINO, R. & UEDA, T. 1985 Studies on heat transfer and flow characteristics in subcooled flow boiling. Part 1: boiling characteristics. Part 2: flow characteristics. *Int. J. Multiphase Flow* **11,** 269–297.

JENS, W. H. & LOTTES, P. A. 1951 Analysis of heat transfer, burnout, pressure drop and density data for high pressure water. USAEC Report ANL-4627, Argonne National Lab., Argonne, Ill.

JIJI, L. & CLARK, J. S. 1964 Bubble boundary layer and temperature profiles for forced convection boiling in channel-flow. *Trans ASME J. Heat Transfer* **86,** 50–61.

KANDLIKAR, S. G. 1989 Development of flow boiling map for subcooled and saturated flow boiling of different fluids inside circular tubes. In *Heat Transfer With Phase Change* (Edited by HABIB, I. S. & DALLMAN, R. M.). *ASME Publication HTD*, Vol. 144. ASME, New York.

KENNING, D. B. R. & COOPER, M. G. 1989 Saturated flow boiling in vertical tubes *Int. J. Heat Mass Transfer* **32,** 445–457.

KREITH, F. & SUMMERFIELD, M. 1949 Heat transfer to water at high flux densities with & without surface boiling. *Trans. ASME* **71,** 805–811.

LAHEY,R. T. JR. & MOODY, F. J. 1977 The thermal hydraulics of a boiling water reactor. *ANS Monogr.* ANS, Hindsdale, Ill.

LEE, S. L. & DURST, F. 1980 On the motion of particles in turbulent flow. U.S. Nuclear Regulatory Commission Report. NUREG/CR-1556.

LEVY, S. 1967 Forced convection subcooled boiling prediction of vapor volume fraction. *Int. J. Heat Mass Transfer* **10,** 951–965.

MULLER-STEINHAGEN, H., EPSTEIN, N. & WATKINSON, A. P. 1986 Subcooled-boiling and convection heat transfer to heptane flowing in an annulus and past a coiled wire. *Trans. ASME J. Heat Transfer* **108,** 922–933.

ROHSENHOW, W. M. 1952 A method of correlating heat transfer data for surface boiling of liquids. *Trans. ASME* **74,** 969–976.

ROUHANI, S. Z. & AXELSON, E. 1970 Calculation of void volume fractions in subcooled and quality boiling regimes. *Int. J. Heat Mass Transfer* **13,** 383–393.

SAHA, P. & ZUBER, N. 1974 Point of net vapor generation and vapor void fraction in subcooled boiling. In *Proc. 5th Int Heat Transfer Conf.*, Tokyo, Paper B4.7.

SHAH, M. M. 1977 A general correlation for heat transfer during subcooled boiling in pipes and annuli. *ASHRAE Trans.* **83,** 202–217.

SKIRPOV, V. K. 1972 *Metastable Liquids.* Nauka, Moscow.

THOM, J. R. S., WALKER, W. M., FELLON, T. A. & REISING, G. F. 1965 Boiling in sub-cooled water during flow up heated tubes or annuli. *Proc. Inst. mech. Engrs* **180,** 226–242.

TONG, L. S., CURRIN, H. B., LARSEN, P. & SMITH, D. G. 1965 Influence of axially non-uniform heat flow on DNB. *AIChE Symp. Ser.* **64,** 35–43.

WEISMAN, J.1988 Letter to editor. *Fusion Technol.* **14,** 1418.

WEISMAN, J. & ILLESLAMLOU, S. 1988 A phenomenological model for prediction of critical heat flux under highly subcooled conditions. *Fusion Technol.* **13,** 654–659.

WEISMAN, J. & PEI, B. S. 1983 Prediction of critical heat flux in flow boiling at low qualities. *Int. J. Heat Mass Transfer* **26,** 1463–1477.

WEISMAN, J. & YING, S. H. 1985 A theoretically based critical heat flux prediction for rod bundles at PWR conditions. *Nucl. Engng Des.* **85,** 239–250.

YAGOV, V. V. & PUZIN, V. A. 1985 Burnout under conditions of force-fed flow of subcooled liquid. *Therm. Engng* **32,** 569–572.

YING, S. H. & WEISMAN, J.1986 Prediction of critical heat flux in flow boiling at intermediate qualities. *Int. J. Heat Mass Transfer* **29,** 1639–1647.